Supplementary Information

Aloe-emodin derived azoles as a new structural type of potential antibacterial agents: Design, synthesis and evaluation of the action on membrane, DNA and MRSA DNA isomerase

Xin-Yuan Liang,[a] Narsaiah Battini,[a,#] Yan-Fei Sui,[a] Mohammad Fawad Ansari,[a,§] Lin-Ling Gan,[b,**] Cheng-He Zhou[a,*]

[a] *Institute of Bioorganic & Medicinal Chemistry, Key Laboratory of Luminescence Analysis and Molecular Sensing (Southwest University), Ministry of Education, School of Chemistry and Chemical Engineering, Southwest University, Tiansheng street 2, Beibei district, Chongqing 400715, PR China.*
[b] *Chongqing Engineering Research Center of Pharmaceutical Sciences, School of Pharmacy, Chongqing Medical and Pharmaceutical College, Chongqing 401331, PR China.*
[**] *Corresponding author: E-mail: ganlinling2012@163.com.*
[*] *Corresponding author. Tel./Fax: +86-023-68254967. E-mail address: zhouch@swu.edu.cn.*
[#] *Postdoctoral fellow from CSIR–Indian Institute of Integrative Medicine (IIIM), Jammu, India.*
[§] *Postdoctoral fellow from Jamia Millia Islamia, New Delhi, India.*

1. Experimental protocols

1.1 General methods

X-6 melting point apparatus was used to measure the melting points. Precoated silica gel plates were used to perform TLC analysis. Bruker AV 600 spectrometer was used to record NMR spectra by treating tetramethylsilane (TMS) as an internal standard. IonSpec FT-ICR mass spectrometer with ESI resource is used to record the high-resolution mass spectra (HRMS). All fluorescence spectra were recorded on F-7000 Spectrofluorimeter (Hitachi, Tokyo, Japan) equipped with 1.0 cm quartz cells, the widths of both the excitation and emission slit were set as 2.5 nm, and the excitation wavelength was 280 nm. Fluorescence spectra were recorded at 290 K in the range of 300–550 nm. The UV spectrums were recorded at room temperature on a TU-2450 spectrophotometer (Puxi Analytic Instrument Ltd. of Beijing, China) equipped with 1.0 cm quartz cells. Tris and HCl were analytical purity. Sample masses were weighed on a microbalance with a resolution of 0.1 mg. All other chemicals and solvents were commercially available, and were used without further purification.

The stock solution of compound **4b** was prepared in DMSO. Calf thymus DNA (Sigma Chemical Co., St. Louis, MO) was used without further purification, and its stock solution was prepared by dissolving an appropriate amount of DNA in doubly distilled water. The solution was allowed to stand overnight and stored at 4 ºC in the dark for about one week. The concentration of DNA in stock solution was determined by UV absorption at 260 nm using a molar absorption coefficient ξ_{260} = 6600 L·mol^{-1}·cm^{-1} (expressed as molarity of phosphate groups) by Bouguer-Lambert-Beer law. The purity of DNA was checked by monitoring the ratio of the absorbance at 260 nm to that at 280 nm. The solution gave a ratio of > 1.8 at A260/A280, which indicated that DNA was sufficiently free from protein. NR stock solution was prepared by dissolving its solid (Sigma Chemical Co.) in doubly distilled water and was kept in a cool and dark place. All the solutions were adjusted with Tris-HCl buffer solution (pH = 7.4), which was prepared by mixing and diluting Tris solution with HCl solution. All chemicals were of analytical reagent grade, and doubly distilled water was used throughout.

1.2. Antibacterial and antifungal assays

In comparison with the bacteria, the tested fungi were less sensitive to target aloe-emodin azoles **3-8**. The target aloe-emodins gave no obvious suppression on *C. albicans* strains, and displayed low activity towards *C. parapsilosis* ATCC 22019, except for 2-mercaptotriazole derivative **7b** (MIC = 16 μg/mL). In addition, as for *C. tropicalis*, aloe-emodins **4a,**

4b and **8** exhibited moderate potency, which might be attributed to the existence of 1,2,4-triazole, non-substituted tetrazole, indole and 2-mercaptobenzimidazole, respectively. Remarkably, all the aloe-emodin azoles showed better activities against *A. fumigatus* (MIC = 4–64 μg/mL) than clinical antifungal fluconazole (MIC = 256 μg/mL), except for 2-mercapto-1-methylimidazole **7a**. It is worth noting that benzotriazolyl aloe-emodin **5e** and 2-mercaptotriazole derivative **7b** possessed prominent suppression on *A. fumigatus* strains with MIC value as low as 4 μg/mL. Therefore, the two compounds are promising to serve as anti-*A. fumigatus* agents to be further exploited.

Table S1. Antifungal data as MIC ($\mu g \cdot mL^{-1}$) for compounds **3-8** .

Compds	Fungi[a]			
	C. a.	*C. t.*	*A. f.*	*C. p.* 22019
2	2	4	4	2
3a	32	32	16	64
3b	64	32	64	64
3c	32	32	8	128
4a	64	16	16	32
4b	64	16	32	64
4c	256	64	64	128
5a	64	32	32	32
5b	64	64	64	128
5c	32	64	64	128
5d	32	64	32	128
5e	64	32	4	64
6	64	64	16	32
7a	256	128	256	128
7b	32	512	4	16
7c	64	64	16	32
8	128	16	32	256
Fluconazole	4	8	256	2

[a] *C. a., Candida albicans*; *C. t.*, *Candida tropicalis*; *A. f., Aspergillus fumigatus*; *C. p.* 22019, *Candida parapsilosis* ATCC 22019.

The prepared compounds were evaluated for their antibacterial activities against Gram-positive bacteria (MRSA, *Enterococcus faecalis*, *Staphylococcus aureus*, *Staphylococcus aureus* ATCC 25923, and *Staphylococcus aureus* ATCC 29213) and Gram-negative bacteria (*Klebsiella pneumoniae*, *Escherichia coli*, *Escherichia coli* ATCC 25922, *Pseudomonas aeruginosa*, *Pseudomonas aeruginosa* ATCC 27853, and *Acinetobacter baumannii*) with the positive control of clinical antibacterial drug norfloxacin. The bacterial suspension was adjusted with sterile saline to a concentration of 1×10^5 CFU. Initially the compounds were dissolved in DMSO to prepare the stock solutions, then the tested compounds and reference drugs were prepared in Mueller-Hinton broth (Guangdong huaikai microbial sci. & tech co., Ltd, Guangzhou, Guangdong, China) to obtain the required concentrations of 512, 256, 128, 64, 32, 16, 8, 4, 2, 1, 0.5 $\mu g \cdot mL^{-1}$. These dilutions were inoculated and incubated at 37 ºC for 24 h. Antibacterial screening demonstrated that some of the target compounds could effectively inhibit the growth of the tested bacteria and exhibit broad antimicrobial spectrum.

Likewise, all the prepared hybrids were tested for their antifungal properties against four fungi (*Candida albicans*, *Candida tropicalis*, *Aspergillus fumigatus*, and *Candida parapsilosis* ATCC 22019) with respect to clinical fluconazole. A spore suspension in sterile distilled water was prepared from one day old culture of the fungi growing on Sabouraud agar (SA) media. The final spore concentration was observed to be $1–5\times10^3$ spore$\cdot mL^{-1}$. Eleven required concentrations

Minimal inhibitory concentration (MIC, μg·mL^{-1}) is defined as the lowest concentration of the new compounds that completely inhibit the growth of fungi, by means of standard two-fold serial dilution method in 96-well microtest plates (0.5–512 μg·mL^{-1}) of each tested compound were prepared by making dilutions in sterile RPMI 1640 medium using compound's stock solutions. These dilutions were inoculated and incubated at 35 ºC for 24 h according to the Clinical & Laboratory Standards Institute (CLSI). The tested microorganism strains were provided by the Clinical Laboratory Department, Sichuan Academy of Medical Sciences & Sichuan Provincial People's Hospital. To ensure that the solvent had no effect on antifungal growth, a control test was performed with test medium supplemented with DMSO at the same dilutions as used in the experiment. All the fungi growth was monitored visually and spectrophotometrically. The lowest concentration (highest dilution) required to arrest the growth of fungi was regarded as minimal inhibitory concentration (MIC).

1.3. Resistance development assay

The representative compound **4b** was selected to investigate the developing rate of bacterial resistance according to the reported method. We exposed a standard strain of resistant MRSA toward increasing concentrations of compound **4b** from sub-MIC (0.5 × MIC, MIC is the minimal inhibitory concentration) for sustained passages and determined the new MIC values of compound **4b** for each passage of MRSA. The initial MIC values of compound **4b** and norfloxacin were determined against MRSA as mentioned above in antibacterial assay. For the next MIC experiment, the bacterial dilution was prepared by using the bacteria from sub-MIC concentration of the compound (0.5 × MIC). After a 12 h incubation period, again bacterial dilution was prepared by using the bacterial suspension from sub-MIC concentration of the compound (0.5×MIC) and assayed for the next MIC experiment. The process was repeated for 15 passages. The MIC values for compound **4b** and norfloxacin against each passage of MRSA were determined.

1.4. Cytotoxicity

Cell viability upon the treatment of the prepared compounds were tested by using the CCK8 assay. Briefly, a suspension of cells (3000/well for normal human liver cell line LO2) were seeded in 96-well plates and cultured for 24 h. Then different concentrations ranging from 100 to 6.25 μM (PBS buffer containing 1% DMSO) for the compound **4b** were added into the 96-well plates, in which cells were incubated for 72 h. Then, 10 μL of CCK8 solution was added to each well of the plates and incubated at 37 ℃ for 2 h. The absorbance of each well was measured at 450 nm in a microplate reader. At last, resultant $OD_{450\ nm}$ values were expressed as IC_{50} values. The anti-tumor growth effects of compound **4b** *in vitro* were studied *via* measuring the viability of Hep-G2 cell using the above approach. The relative inhibition rates of cancer cell growth and IC_{50} values were calculated and plotted by GraphPad Prism6. Experiments were repeated at least three times.

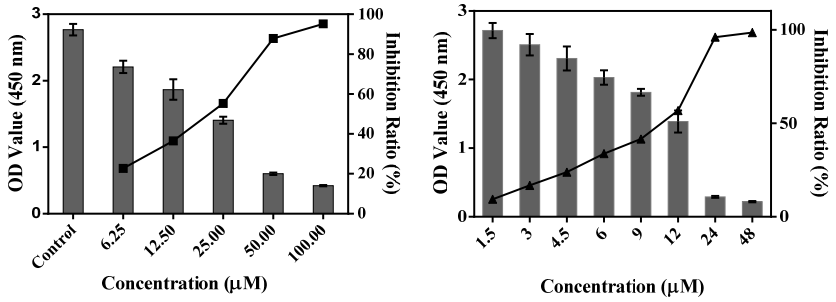

Figure S1. Cytotoxic assay of the active compound **4b** on human hepatocyte LO2 cell line, IC_{50} = 26.62, selectivity index = 11.76 (left)

and hepatoma Hep-G2 cell line, IC_{50} = 11.76, selectivity index = 1.96 (right).

1.5. ROS generation

Intracellular ROS was measured using standard 2,7-dichlorofluoroscein diacetate (DCFH-DA) assay. Then 10^6 CFU/mL of MRSA strain cells were treated with increasing concentrations of compound **4b** for 6 h at 37 °C. Following treatment, both control and treated cells were washed with PBS and incubated with 10 μM DCFH-DA probe for 30 min in dark at 37 °C. The green fluorescence originating from the oxidative cleavage of DCFH-DA to DCF was measured with an excitation wavelength of 485 nm and emission wavelength of 528 nm. The fold increase in intracellular ROS production in cells treated with compound **4b** in comparison to control cells was plotted.

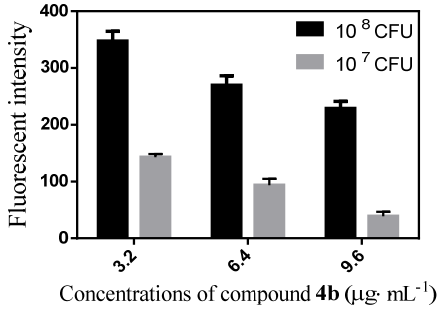

Figure S2. Changes of ROS level in MRSA treated by compound **4b** (12× MIC).

1.6. Bacterial membrane permeabilization

The overnight grown culture of MRSA was harvested (10000 rpm, 1 min), washed, and resuspended in 5 mM glucose and 5 mM HEPES buffer (pH = 7.4) in 1:1 ratio. Then an amount of 10 μL of test compound **4b** (12 × MIC) was added to a cuvette containing 2 mL of bacterial suspension and 10 μM propidium iodide (PI). Fluorescence was monitored at excitation wavelength of 535 nm (slit width of 10 nm) and emission wavelength of 617 nm (slit width of 5 nm). A control experiment was performed by treating the preincubated bacterial and dye solution only with water (10 μL).

1.7. Fluorescence microscopy

The overnight grown culture of MRSA was treated with compound **4b** (12 × MIC), and 0.1% Triton X-100 was used as positive control. All the treated and untreated cells (as negative control) were washed once with 1 × PBS (the images were captured with a 10 × objective in electron microscope) and stained with 4.5 mM PI for 15 min at 37 ºC Finally, the images were captured with a 10 × objective in fluorescence microscope using green light.

1.8. Interactions with calf thymus DNA

DNA is an informational molecule encoding the genetic information, which makes it one of the objectives for the studies of biologically important small molecules such as antimicrobial drugs. Recently, DNA is increasingly investigated for interaction with small molecules in the rational design and construction of novel and efficient drugs. To explore the possible antimicrobial action mechanism, calf thymus DNA was selected as DNA model because of its medical importance, low cost and ready availability properties to study the binding behavior of compound **4b** with calf thymus DNA on molecular level using neutral red (NR) dye as a spectral probe *in vitro* by UV-vis spectroscopic methods.

1.8.1. Absorption spectra of DNA in the presence of compound 4b

In this study, UV–vis absorption spectra were documented while the concentration of DNA being fixed with the consecutive and proportional increase of the concentration of compound **4b**. As demonstrated in Fig. S3, the UV-vis absorption of DNA was first observed at 260 nm which showed gradual increase in absorbance associated by a slight red shift with the raising concentration of compound **4b**. Moreover, the absorbance of **4b**–DNA complex (inset of Fig. S2) was recorded less than that of the sum of free DNA and free compound **4b**, which signified that a weak hypochromic effect has occurred between the CT-DNA and compound **4b**. Both the hypochromic effect and hypochromic region preliminarily disclosed that the interaction mode of compound **4b** was the intercalation into DNA, which were in accordance with the displayed spectral changes.

On the base of variations in the absorption spectra of DNA upon binding to compound **4b**, equation (1) can be utilized to calculate the binding constant (*K*).

$$\frac{A^0}{A-A^0}=\frac{\xi_C}{\xi_{D-C}-\xi_C}+\frac{\xi_C}{\xi_{D-C}-\xi_C}\times\frac{1}{K[Q]} \qquad (1)$$

A^0 refers to the absorbance of DNA in the absence of compound **4b** while A refers to the absorbance in the presence of **4b** at 260 nm. In addition, ξ_C and $\xi_{D\text{-}C}$ represents the absorption coefficients of compound **4b** and compound **4b**–**DNA** complex respectively. Also, [Q] stands for the volumetric molar concentration of compound **4b** measured as mol·L^{-1} unit. The plot of $A^0/(A–A^0)$ vs 1/[compound **4b**] is plotted by making use of the absorption titration data and linear fitting (Fig. S4), binding constant, K = 3.421 × 10^5 L·mol^{-1}, (R = 0.990, SD = 0.008). Here, R is the correlation coefficient while SD refers to standard deviation. (R is the correlation coefficient, and SD is standard deviation).

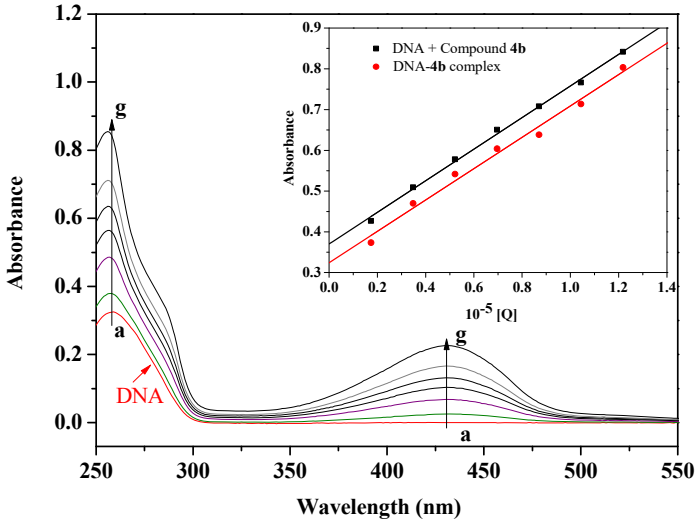

Figure S3. UV absorption spectra of DNA with different concentrations of compound **4b** (pH = 7.4, T = 290 K). Inset: comparison of absorption at 2

60 nm between the compound **4b**–DNA complex and the sum values of free DNA and free compound **4b**. c(DNA)= 5.25 × 10^{-5} mol·L^{-1}, and c(compound **4b**) = 0–1.25 × 10^{-5} mol·L^{-1} for curves **a–g** respectively at increment 0.25 × 10^{-5}

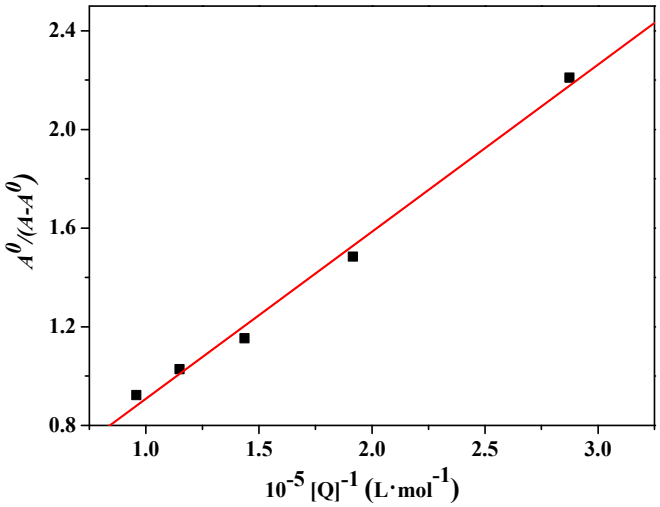

Figure S4. The plot of $A^0/(A-A^0)$ versus 1/[compound **4b**]

1.8.2. Absorption spectra of NR interactions with DNA

To further understand the interaction between compound **4b** and DNA, the absorption spectra of competitive interaction of compound **4b** with Neutral Red (NR) were investigated. NR is a planar phenazine dye possessing a higher stability, lower toxicity and more convenient application, compared with other common probes. Furthermore, the binding of NR with DNA is an intercalative mode which has been sufficiently demonstrated. Therefore, NR was used as a spectral probe to investigate the binding mode of **4b** with DNA in the present work. The absorption spectra of the NR dye upon the addition of DNA are depicted in Fig. S5. Apparently, the absorption peak of the NR at around 460 nm showed gradual decrease with the increasing concentration of DNA, and a new band at around 530 nm developed. This could be attributed to the formation of the new DNA–NR complex. An isosbestic point at 504 nm provided additional evidence of DNA–NR complex formation.

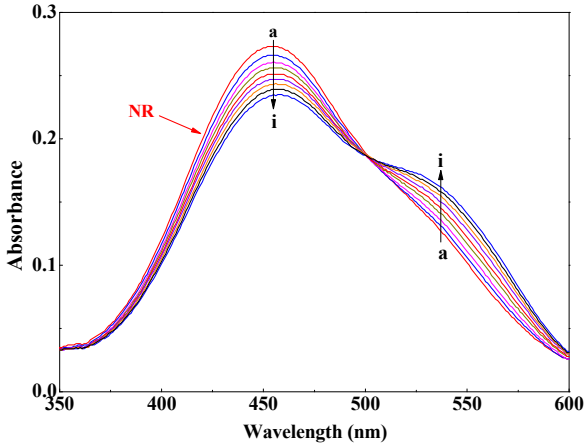

Figure S5. UV absorption spectra for NR and DNA (pH = 7.4, T = 298 K). c(NR) = 2 × 10^{-5} mol·L^{-1}, and c(DNA) = 0–3.81 × 10^{-5} mol·L^{-1} at an increment of 0.48 × 10^{-5} for curves *a–i* respectively.

1.9. Molecular docking

To further understand the mechanism of action of the synthesized compounds, highly active molecule **4b** was docked

into the active site of MRSA DNA isomerase (PDB code: 2XCS). Sybyl 2.0 and Pymol 4.5.0 was used to perform the docking work. The gird size was set to be 45 × 45 × 45 and the grid point spacing was set at default value 0.375 Å. The Lamarkian genetic algorithm (LGA) was applied for the conformational search.

1.10. General procedure and spectral data for some prepared compounds

*1.10.1. Synthesis of 3-(chloromethyl)-1,8-dihydroxyanthracene-9,10-dione (**2**)*

Aloe emodin (**1**) (2.70 g, 10 mmol) was dissolved in 200 mL anhydrous *N, N*-dimethylformamide, and sulfoxide chloride (20 mL, 275 mmol) was slowly dropped in an ice bath. After stirring for 1 h, the reaction was removed from the ice bath at room temperature. TLC was followed until the end of the reaction. The compound **2** was quenched with ice water, filtered, washed and recrystallized. Yield: 61.0%, melting point: 138−140 ºC.

*1.10.2. Synthesis of 1,8-dihydroxy-3-((2-nitro-1H-imidazol-1-yl)methyl)anthracene-9,10-dione (**3a**)*

A mixture of 2-nitroimidazole (84 mg, 0.75 mmol) and potassium carbonate (138 mg, 1.00 mmol) were stirred in acetonitrile (10 mL) at 65 °C. Compound **2** (144 mg, 0.50 mmol) was added and reflux was performed at 80 °C. Thin-layer chromatography was followed until the end of the reaction. After cooling to room temperature and neutralizing with glacial acetic acid until pH was neutral, the filtrate was then extracted and purified by column chromatography (Eluent: petroleum ether/ethyl acetate (10/1−10/3, V/V)), the compound **3a** (40 mg) was obtained as yellow solid, yield: 22.4%, melting point: >250 °C. ^{1}H NMR (600 MHz, DMSO-d_6) δ 11.97 (s, 2H, anthraquinone-1,8-O*H*), 8.46 (s, 1H, imidazole-4-*H*), 8.15 (s, 1H, imidazole-5-*H*), 7.86 (d, *J* = 7.7 Hz, 1H, anthraquinone-5-*H*), 7.84 (s, 1H, anthraquinone-4-*H*), 7.83 (d, *J* = 8.2 Hz, 1H, anthraquinone-7-*H*), 7.78 (d, *J* = 7.4 Hz, 1H, anthraquinone-6-*H*), 7.44 (s, 1H, anthraquinone-2-*H*), 5.75 (s, 2H, CH_2); ^{13}C NMR (151 MHz, DMSO-d_6) δ 191.98, 181.67, 161.93, 147.84, 146.20, 138.15, 137.96, 134.40, 133.73, 125.03, 123.50, 122.13, 119.89, 118.78, 116.36, 50.55; HRMS (ESI) calcd. for $C_{18}H_{11}N_3O_6$ $[M+H]^+$: 366.0726; found, 366.0725.

The preparation method of compound **3b-8** is the same as that of compound **3a**.

*1.10.3. Synthesis of 1,8-dihydroxy-3-((4-nitro-1H-imidazol-1-yl)methyl)anthracene-9,10-dione (**3b**)*

Yellow solid, yield: 60.4%, melting point: >250 °C; ^{1}H NMR (600 MHz, DMSO-d_6) δ 11.90 (s, 2H，anthraquinone-1,8-O*H*), 8.59 (s, 1H, imidazole-5-C*H*), 8.09 (s, 1H, imidazole-2-C*H*), 7.81 (t, *J* = 7.9 Hz, 1H, 6-C*H*), 7.71–7.68 (m, 2H, anthraquinone-4,5-2C*H*), 7.40 (d, *J* = 8.2 Hz, 1H, anthraquinone-7-C*H*), 7.38 (d, *J* = 10.0 Hz, 1H, anthraquinone-2-C*H*), 5.46 (s, 2H, CH_2); ^{13}C NMR (151 MHz, DMSO-d_6) δ 191.98, 181.67, 161.93, 147.84, 146.20, 138.15, 137.96, 134.40, 133.74, 125.01, 123.49, 122.13, 119.89, 118.78, 116.36, 50.52; HRMS (ESI) calcd. for $C_{18}H_{11}N_3O_6$ $[M+H]^+$: 366.0726; found, 366.0725.

*1.10.4. Synthesis of 1,8-dihydroxy-3-((2-methyl-5-nitro-1H-imidazol-1-yl)methyl)anthracene-9,10-dione (**3c**)*

Yellow solid, yield: 31.1%, melting point: >250 °C; ^{1}H NMR (600 MHz, DMSO-d_6) δ 11.95 (s, 2H, anthraquinone-1,8-O*H*), 10.14 (s, 1H, imidazole-4-*H*), 8.15 (s, 1H, anthraquinone-4-*H*), 7.87 (d, *J* = 8.1 Hz, 1H, anthraquinone-5-*H*), 7.85 (d, *J* = 4.9 Hz, 1H, anthraquinone-7-*H*), 7.79 (t, *J* = 7.1 Hz, 1H, anthraquinone-6-*H*), 7.44 (d, *J* = 8.4 Hz, 1H, anthraquinone-2-*H*), 5.33 (d, *J* = 4.6 Hz, 1H, CH_2), 5.23 (s, 1H, CH_2), 1.24 (s, 3H, CH_3); ^{13}C NMR (151 MHz, DMSO-d_6) δ 161.87, 144.96, 137.96, 134.38, 125.02, 123.70, 119.90, 118.84, 116.42, 79.63, 40.53, 12.91; HRMS (ESI) calcd. for $C_{16}H_{10}N_4O_4$ [M + H]$^+$, 323.0780; found, 323.0782.

*1.10.5. Synthesis of 3-((1H-1,2,4-triazol-1-yl)methyl)-1,8-dihydroxyanthracene-9,10-dione (**4a**)*

Yellow solid, yield: 46.2%, melting point: >250 °C; ^{1}H NMR (600 MHz, DMSO-d_6) δ 12.05 (s, 1H, anthraquinone-8-O*H*), 11.98 (s, 1H, anthraquinone-1-O*H*), 8.21 (s, 1H, triazole-5-*H*), 8.04 (s, 1H, triazole-3-*H*)), 7.84 (d, *J* = 7.2 Hz, 1H, anthraquinone-5-*H*), 7.70 (d, *J* = 7.9 Hz, 2H, anthraquinone-6,4-2*H*), 7.32 (d, *J* = 8.4 Hz, 1H, anthraquinone-7-*H*), 7.09 (s, 1H, anthraquinone-2-*H*), 5.45 (s, 2H, CH_2); ^{13}C NMR (151 MHz, $CDCl_3$) δ 194.62–188.82, 162.99, 152.81, 145.98–141.91, 137.47, 135.29–131.60, 124.93, 122.89, 120.28, 118.60, 52.67; HRMS (ESI) cald. for $C_{17}H_{11}N_3O_4$ [M+H]$^+$: 322.0828; found, 322.0819.

*1.10.6. Synthesis of 3-((1H-tetrazol-1-yl)methyl)-1,8-dihydroxyanthracene-9,10-dione (**4b**)*

Yellow solid, yield: 49.2%, melting point: >250 °C; ^{1}H NMR (600 MHz, $CDCl_3$) δ 12.04 (s, 1H, anthraquinone-8-O*H*), 11.95 (s, 1H, anthraquinone-1-O*H*), 8.59 (s, 1H, tetrazole-5-*H*), 7.84 (s, 1H, anthraquinone-4-*H*), 7.77 (d, *J* = 7.5 Hz, 1H, anthraquinone-5-*H*), 7.70 (s, 1H, anthraquinone-7-*H*), 7.32 (dd, *J* = 8.5, 2.4 Hz, 1H, anthraquinone-6-*H*), 7.18 (s, 1H, anthraquinone-2-*H*), 5.90 (s, 2H, CH_2); ^{13}C NMR (151 MHz, $CDCl_3$) δ 161.87, 144.96, 137.96, 134.38, 125.02, 123.70, 119.90, 118.84, 116.42, 55.32; HRMS (ESI) calcd. for $C_{16}H_{10}N_4O_4$ [M+H]$^+$, 323.0780; found, 323.0783.

*1.10.7. Synthesis of 1,8-dihydroxy-3-((5-methyl-1H-tetrazol-1-yl)methyl)anthracene-9,10-dione (**4c**)*

Yellow solid, yield: 42.1%, melting point: >250 °C; ^{1}H NMR (600 MHz, DMSO-d_6) δ 11.90 (s, 2H, anthraquinone-1,8-O*H*), 7.81 (s, 1H, anthraquinone-4-*H*), 7.71 (s, 1H, anthraquinone-5-*H*), 7.53 (d, *J* = 1.3 Hz, 1H, anthraquinone-6-*H*), 7.40 (s, 1H, anthraquinone-7-*H*), 7.22 (s, 1H, anthraquinone-2-*H*), 5.82 (s, 2H, CH_2), 2.55 (s, 3H, CH_3); ^{13}C NMR (151 MHz, DMSO-d_6) δ 161.89, 119.89, 49.43, 14.54; HRMS (ESI) calcd. for $C_{17}H_{13}N_4O_4$ [M+H]$^+$: 337.0937; found, 337.0938.

*1.10.8. Synthesis of 3-((1H-benzo[d]imidazol-1-yl)methyl)-1,8-dihydroxyanthracene-9,10-dione (**5a**)*

Yellow solid, yield: 61.1%, melting point: >250 °C; ^{1}H NMR (600 MHz, DMSO-d_6) δ 11.90 (s, 2H, anthraquinone-1,8-O*H*), 8.50 (s, 1H, benzomidazole-2-C*H*), 7.78 (s, 1H, anthraquinone-4-C*H*), 7.71 (d, *J* = 7.2 Hz, 1H, anthraquinone-5-C*H*), 7.67 (s, 1H, benzomidazole-4-C*H*), 7.57–7.53 (m, 2H, anthraquinone-6,7-2C*H*), 7.37 (s, 1H, anthraquinone-2-C*H*), 7.23 (dd, *J* = 8.9, 3.4 Hz, 3H, benzomidazole-5,6,7-3C*H*), 5.69 (s, 2H, CH_2); ^{13}C NMR (151 MHz,

DMSO-d_6) δ191.88, 181.57, 161.89 (d, J = 15.8 Hz), 146.02, 137.15, 125.03, 123.43, 122.12, 119.87, 118.78, 119.89, 49.43; HRMS (ESI) calcd. for $C_{22}H_{14}N_2O_4$ [M+H]$^+$: 371.1032; found, 371.1031.

*1.10.9. Synthesis of 3-((2-ethyl-1H-benzo[d]imidazol-1-yl)methyl)-1,8-dihydroxyanthracene-9,10-dione (**5b**)*

Yellow solid, yield: 31.5%, melting point: >250 °C; ^{1}H NMR (600 MHz, DMSO-d_6) δ 7.81–7.77 (m, 1H, anthraquinone-6-*H*), 7.67 (d, J = 6.8 Hz, 1H, anthraquinone-5-*H*), 7.63 (dd, J = 5.2, 3.7 Hz, 1H, benzoimidazole-4-*H*), 7.48 (dd, J = 5.3, 3.7 Hz, 1H, benzoimidazole-7-*H*), 7.20 (dd, J = 9.0, 5.2 Hz, 2H, benzoimidazole-5, 6-2*H*), 6.97 (s, 1H, anthraquinone-2-*H*), 5.68 (s, 2H, CH_2), 2.74 (dd, J = 12.2, 6.1 Hz, 2H, CH_3CH_2), 1.30 (t, J = 7.4 Hz, 3H, CH_3); ^{13}C NMR (151 MHz, DMSO-d_6) δ 191.98, 181.67, 161.93, 147.02, 138.15, 137.96, 125.01, 123.49, 122.13, 119.89, 118.78, 50.52, 21.54, 11.81; HRMS (ESI) calcd. for $C_{24}H_{18}N_2O_4$ [M+H]$^+$: 399.1345; found, 399.1346.

*1.10.10. Synthesis of 3-((5,6-dimethyl-1H-benzo[d]imidazol-1-yl)methyl)-1,8-dihydroxyanthracene-9,10-dione (**5c**)*

Yellow solid, yield: 28.8%, melting point: >250 °C; ^{1}H NMR (600 MHz, DMSO-d_6) δ 11.90 (s, 1H, anthraquinone-8-O*H*), 11.88 (s, 1H, anthraquinone-1-O*H*), 8.33 (s, 1H, benzoimidazole-2-*H*), 7.82–7.77 (m, 1H, anthraquinone-6-*H*), 7.68 (dd, J = 7.5, 1.0 Hz, 1H, anthraquinone-5-*H*), 7.52 (t, J = 4.4 Hz, 1H, anthraquinone-7-*H*), 7.46 (s, 1H, anthraquinone-4-*H*), 7.37 (d, J = 1.1 Hz, 1H, benzoimidazole-4-*H*), 7.31 (s, 1H, anthraquinone-2-*H*), 7.16 (d, J = 1.5 Hz, 1H, benzoimidazole-7-*H*), 5.62 (s, 2H, CH_2), 1.26–1.23 (s, 6H, CH_3); ^{13}C NMR (151 MHz, DMSO-d_6) δ 191.09, 180.21, 161.46, 161.06, 144.73, 140.89, 139.44, 136.90, 136.10, 134.05, 132.97, 132.25, 132.05, 131.22, 130.46, 129.87, 123.51, 120.64, 118.82, 118.13, 116.67, 114.37, 114.22, 112.95, 108.89, 48.17, 18.92, 18.76; HRMS (ESI) calcd. for $C_{24}H_{18}N_2O_4$ [M+H]$^+$: 399.1345; found, 399.1344.

*1.10.11. Synthesis of 1,8-dihydroxy-3-((5-nitro-1H-benzo[d]imidazol-1-yl)methyl)anthracene-9,10-dione (**5d**)*

Yellow solid, yield: 27.2%, melting point: >250 °C; ^{1}H NMR (600 MHz, DMSO-d_6) δ 11.91 (s, 2H, anthraquinone-1,8-O*H*), 7.89 (s, 1H, benzimidazole-5-C*H*), 7.83–7.80 (m, 1H, anthraquinone-5-C*H*), 7.71 (d, J = 7.4 Hz, 1H, benzimidazole-7-C*H*), 7.54 (d, J = 1.2 Hz, 1H, anthraquinone-4-C*H*), 7.40 – 7.39 (m, 1H, anthraquinone-6-C*H*), 7.30 (s, 1H, benzimidazole-4-C*H*), 7.18 (s, 1H, anthraquinone-7-C*H*), 7.00 (s, 1H, anthraquinone-2-C*H*), 5.39 (s, 2H); ^{13}C NMR (151 MHz, DMSO-d_6) δ 192.01, 181.76, 162.04, 161.83, 148.28, 137.92, 134.23, 133.77, 124.98, 122.74, 119.88, 118.34, 116.45, 49.39, 21.34; HRMS (ESI) calcd. for $C_{22}H_{13}N_3O_6$ [M+H]$^+$: 416.0883; found, 416.0886.

*1.10.12. Synthesis of 3-((1H-benzo[d][1,2,3]triazol-1-yl)methyl)-1,8-dihydroxyanthracene-9,10-dione (**5e**)*

Yellow solid, yield: 22.1%, melting point: >250 °C; ^{1}H NMR (600 MHz, DMSO-d_6) δ 12.02 (s, 1H, 8-O*H*), 11.98 (s, 1H, anthraquinone-1-O*H*), 7.88 (dd, J = 6.6, 3.1 Hz, 2H, benzotriazole-4,7-2C*H*), 7.82 (d, J = 7.5 Hz, 2H, anthraquinone-4,5-C*H*), 7.68 (t, J = 8.0 Hz, 1H, anthraquinone-6-C*H*), 7.41 (dd, J = 6.6, 3.1 Hz, 2H, benzotriazole-5,6-2C*H*), 7.30 (d, J = 8.4 Hz, 1H, anthraquinone-7-C*H*), 7.17 (s, 1H, anthraquinone-2-C*H*), 5.97 (s, 2H, CH_2); ^{13}C NMR (151 MHz, $CDCl_3$) δ 192.64, 181.19, 162.88, 162.65, 144.89, 144.53, 137.38, 134.18, 133.47, 126.86,

124.80, 123.34, 120.18, 119.23, 118.20, 115.73, 59.38; HRMS (ESI) calcd. for $C_{21}H_{13}N_3O_4$ $[M+H]^+$: 372.0984; found, 372.0985.

*1.10.13. Synthesis of 3-((9H-carbazol-9-yl)methyl)-1,8-dihydroxyanthracene-9,10-dione (**6**)*

Yellow solid, yield: 19.1%, melting point: >250 °C; ^{1}H NMR (600 MHz, $CDCl_3$) δ 11.98 (s, 1H, anthraquinone-8-O*H*), 11.95 (s, 1H, H, anthraquinone-1-O*H*), 8.13 (d, *J* = 7.7 Hz, 2H, carbazolyl-4,5-2C*H*), 7.80 (d, *J* = 7.5 Hz, 1H，carbazolyl-1,8-2C*H*), 7.77 (s, 1H，anthraquinone-4-C*H*), 7.66 (t, *J* = 8.0 Hz, 1H，anthraquinone-6-C*H*), 7.44 (t, *J* = 7.7 Hz, 2H，carbazolyl-2,7-2C*H*), 7.31 (d, *J* = 8.2 Hz, 2H，anthraquinone-5,7-2C*H*), 7.29 (d, *J* = 1.7 Hz, 1H, carbazolyl-1-C*H*), 7.27 (d, *J* = 7.9 Hz, 2H, carbazolyl-3,6-C*H*), 6.86 (s, 1H, anthraquinone-2-C*H*), 5.56 (s, 2H, CH_2); ^{13}C NMR (151 MHz, DMSO-d_6) δ 192.89–190.02, 182.50–179.33, 162.08–161.37, 140.56, 138.02–137.62, 134.33–133.22, 130.32–129.75, 126.53, 125.12–124.55, 122.85, 122.14–121.43, 120.96, 118.04–116.91, 116.61–112.85, 109.90, 45.75; HRMS (ESI) calcd. for $C_{27}H_{17}NO_4$ $[M+H]^+$: 420.1236; found, 420.1233.

*1.10.14. Synthesis of 1,8-dihydroxy-3-(((1-methyl-1H-imidazol-2-yl)thio)methyl)anthracene-9,10-dione (7**a**)*

Yellow solid, yield: 51.0%, melting point: >250 °C; ^{1}H NMR (600 MHz, DMSO-d_6) δ 11.94 (s, 1H, anthraquinone-8-O*H*), 11.85 (s, 1H, anthraquinone-1-O*H*), 7.81 (t, *J* = 7.9 Hz, 1H, anthraquinone-6-*H*), 7.71 (d, *J* = 7.5 Hz, 1H, anthraquinone-5-*H*), 7.63 (s, 1H, anthraquinone-4-*H*), 7.39 (d, *J* = 8.3 Hz, 1H, imidazole-5-C*H*), 7.24 (s, 1H, imidazole-4-C*H*), 7.16 (s, 1H, anthraquinone-7-*H*), 6.98 (s, 1H, anthraquinone-2-*H*), 4.31 (s, 2H, CH_2), 3.45 (s, 3H, imidazole -1-CH_3); ^{13}C NMR (151 MHz, DMSO-d_6) δ 194.32–187.39, 183.70–179.03, 161.79, 151.40–147.41, 137.86, 133.79, 129.70, 124.57, 120.13, 115.28, 40.57–39.31, 37.97; HRMS (ESI) calcd. for $C_{19}H_{14}N_2O_4S$ $[M+H]^+$: 367.0753; found, 367.0752.

*1.10.15. Synthesis of 3-(((4H-1,2,4-triazol-3-yl)thio)methyl)-1,8-dihydroxyanthracene-9,10-dione (7**b**)*

Yellow solid, yield: 43.1%, melting point: >250 °C; ^{1}H NMR (600 MHz, DMSO-d_6) δ 12.02 (s, 1H, anthraquinone-8-O*H*), 12.01 (s, 1H, anthraquinone-1-O*H*), 7.98 (s, 1H, triazole-1-*H*), 7.38 (s, 1H, triazole-5-*H*), 7.26 (d, *J* = 25.9 Hz, 3H, anthraquinone-4,5,6-3*H*), 6.95 (s, 1H, anthraquinone-7-*H*), 6.86 (s, 1H, anthraquinone-2-*H*), 4.19 (s, 2H, CH_2); ^{13}C NMR (151 MHz, $CDCl_3$) δ 164.65–161.79, 149.67–145.37, 137.36, 135.29–132.12, 120.21, 119.76, 116.61–114.28, 44.60; HRMS (ESI) calcd. for $C_{17}H_{11}N_3O_4S$ $[M+H]^+$: 354.0549; found, 354.0542.

*1.10.16. Synthesis of 1,8-dihydroxy-3-(((1-methyl-1H-tetrazol-5-yl)thio)methyl)anthracene-9,10-dione (7**c**)*

Yellow solid, yield: 60.1%, melting point: >250 °C; ^{1}H NMR (600 MHz, $CDCl_3$) δ 11.92 (s, 1H, anthraquinone-8-O*H*), 11.94 (s, 1H, anthraquinone-1-O*H*), 7.87 (d, *J* = 1.5 Hz, 1H, anthraquinone-5-*H*), 7.83 (dd, *J* = 7.5, 0.9 Hz, 1H, anthraquinone-6-*H*), 7.70 (s, 1H, anthraquinone-4-*H*), 7.31 (dd, *J* = 8.4, 0.9 Hz, 1H, anthraquinone-7-*H*), 7.26 (s, 1H, anthraquinone-2-*H*), 4.61 (s, 2H, CH_2), 3.91 (s, 3H, tetrazole-5-CH_3); ^{13}C NMR (151 MHz, DMSO-d_6) δ 191.90, 181.62, 161.89, 144.55, 137.95, 134.39, 133.69, 125.03, 123.25, 119.89, 118.47, 116.38, 31.40, 31.11; HRMS (ESI) calcd. for

$C_{17}H_{12}N_4O_4S$ $[M+H]^+$: 369.0658; $[M+Na]^+$: 391.0477; found, 391.0478.

*1.10.17. Synthesis of 3-(((1H-benzo[d]imidazol-2-yl)thio)methyl)-1,8-dihydroxyanthracene-9,10-dione (**8**)*

Yellow solid, yield: 34.1%, melting point: >250 °C; ^{1}H NMR (600 MHz, $CDCl_3$) δ 12.51 (s, 1H, benzomidazole-1-N*H*), 11.92 (s, 1H, anthraquinone-8-O*H*), 11.87 (s, 1H, anthraquinone-1-O*H*), 7.82–7.78 (m, 1H, anthraquinone-4-*H*), 7.70 (dd, *J* = 7.5, 3.5 Hz, 1H, anthraquinone-6-*H*), 7.53–7.49 (m, 2H, benzomidazole-4,7-2*H*), 7.48 (s, 1H, anthraquinone-5-*H*), 7.38 (dd, *J* = 8.4, 2.5 Hz, 1H, anthraquinone-7-*H*), 7.24–7.17 (m, 3H, anthraquinone-2-*H*, benzomidazole-5,6-2*H*), 4.74 (d, *J* = 13.6 Hz, 2H, CH_2); ^{13}C NMR (151 MHz, $CDCl_3$) δ 192.53, 181.97–178.81, 162.72 153.73–150.87 (m), 145.99, 137.34, 124.83, 124.50, 120.24, 115.39, 34.67; HRMS (ESI) calcd. for $C_{22}H_{14}N_2O_4S$ $[M+H]^+$: 403.0753; found, 403.0753.

1.11. Some representative Spectra

^{1}H NMR spectrum of compound **3b**

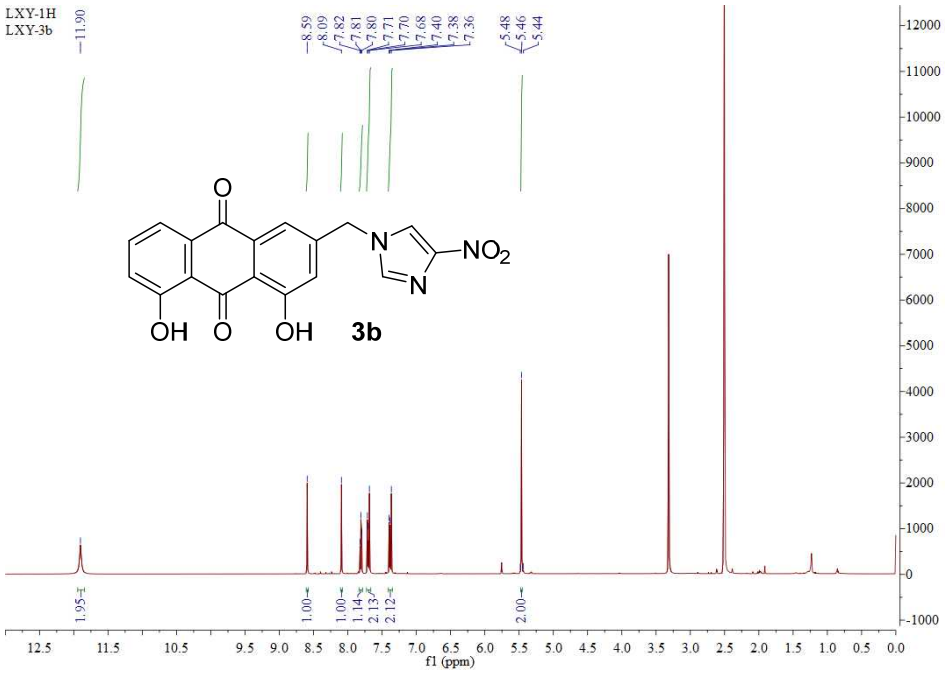

^{13}C NMR spectrum of compound **3b**

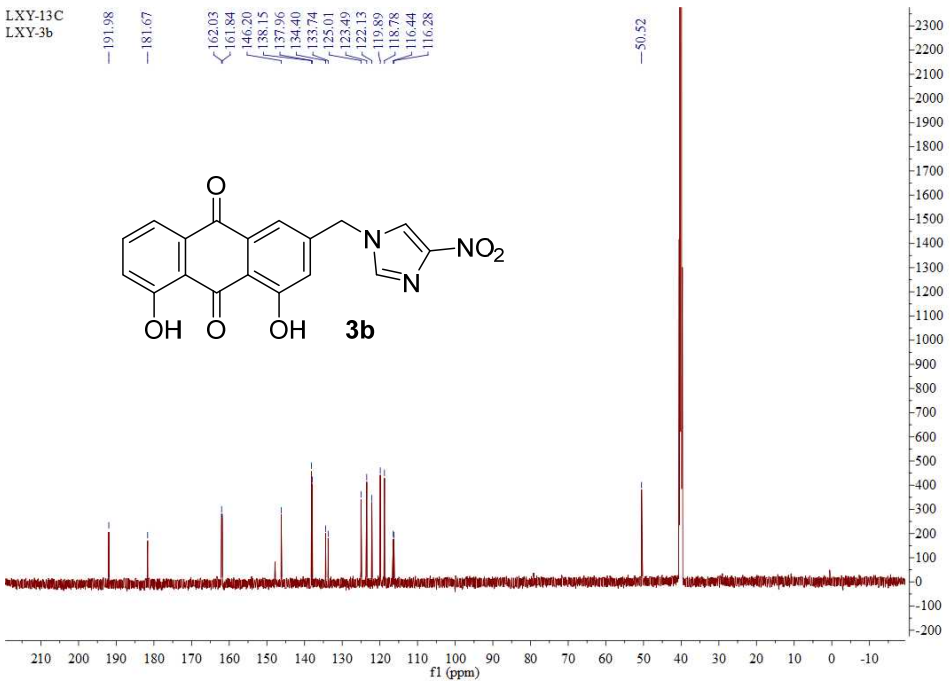

HRMS spectrum of compound **3b**

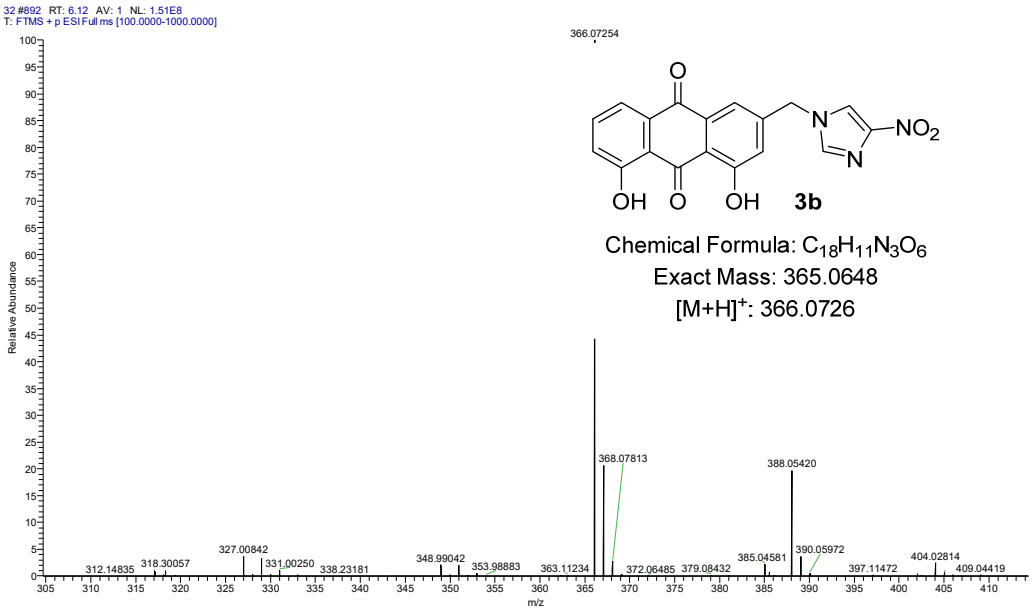

^{1}H NMR spectrum of compound **4a**

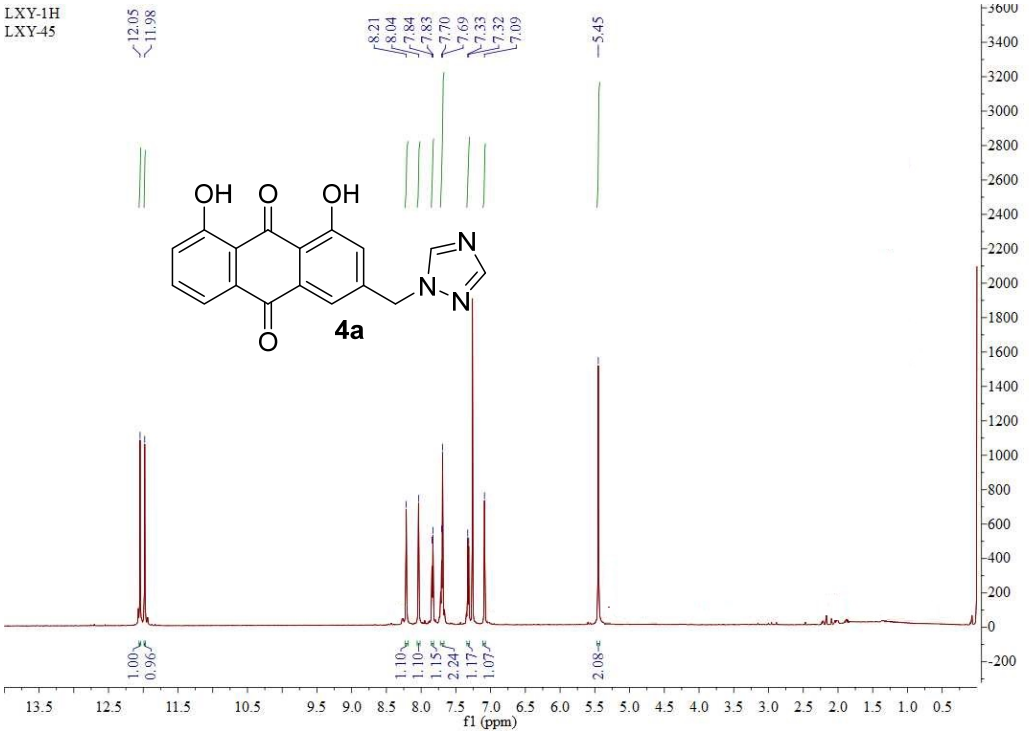

^{13}C NMR spectrum of compound **4a**

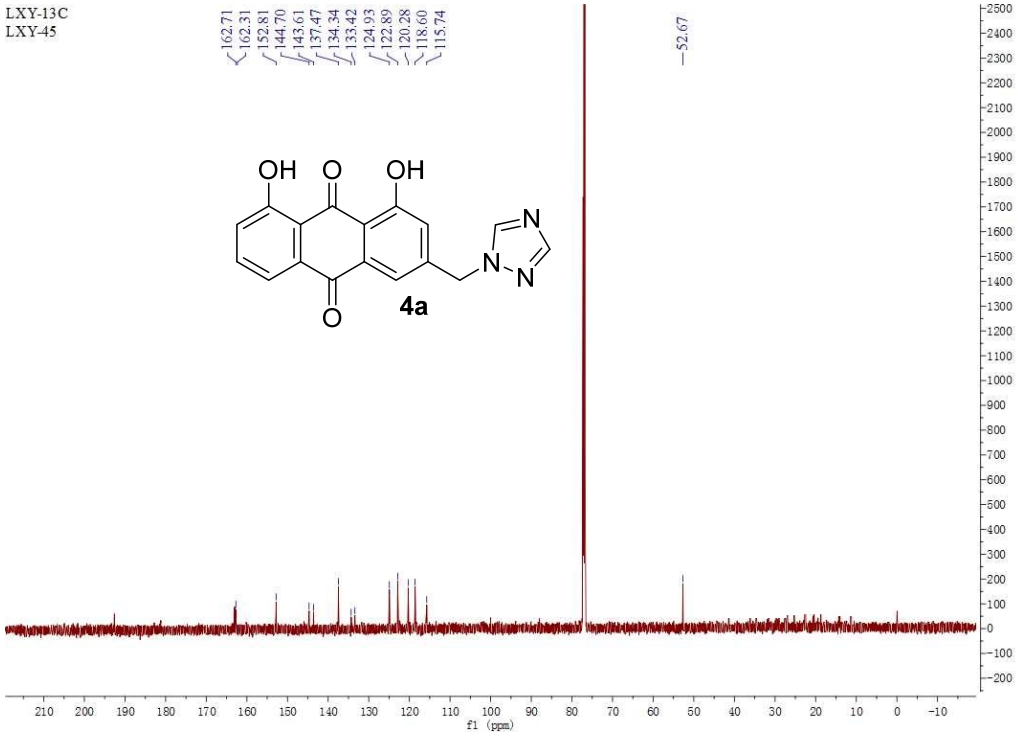

HRMS spectrum of compound **4a**

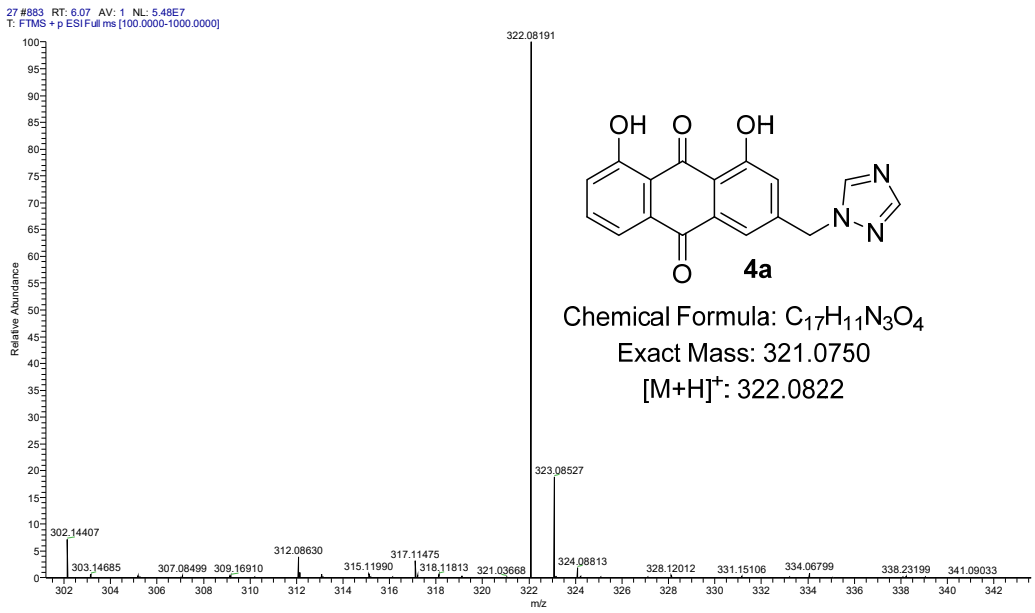

^{1}H NMR spectrum of compound **4b**

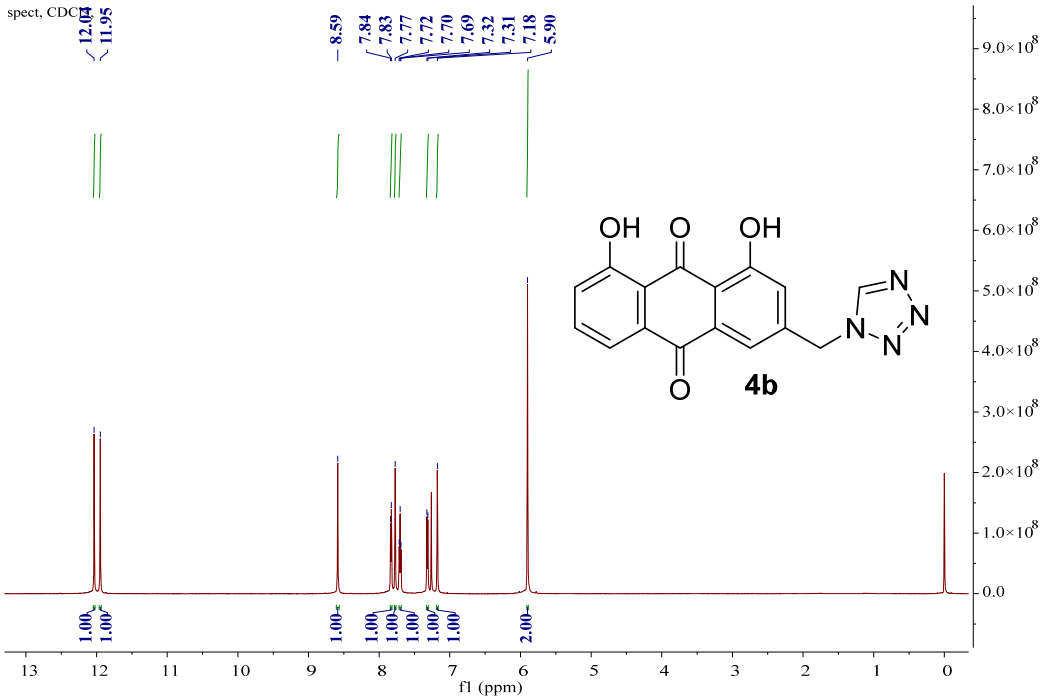

^{13}C NMR spectrum of compound **4b**

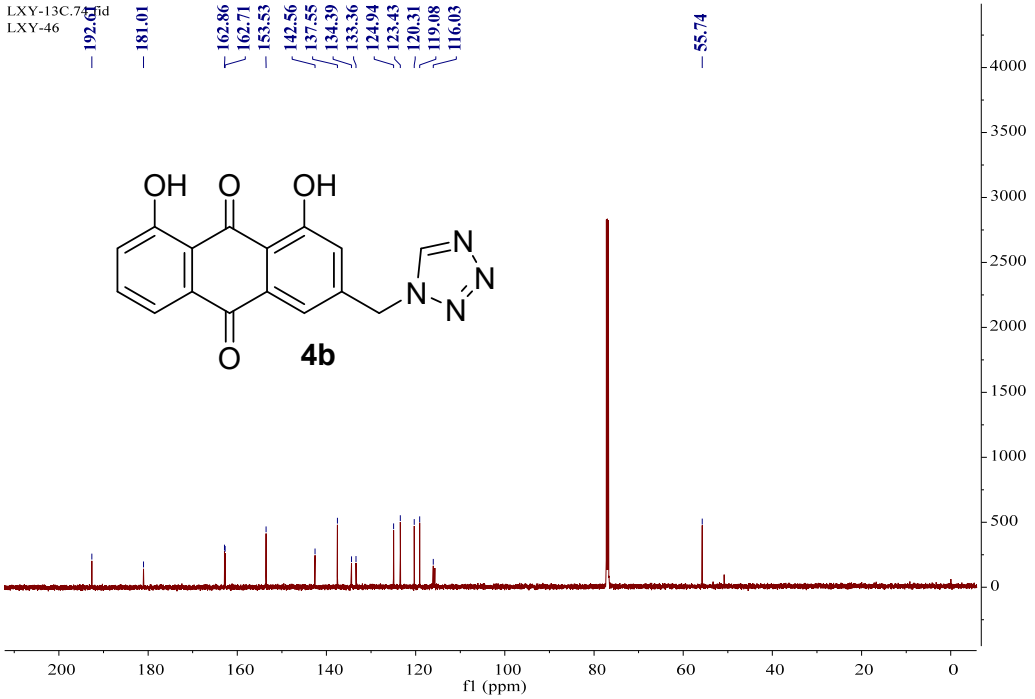

HRMS spectrum of compound **4b**

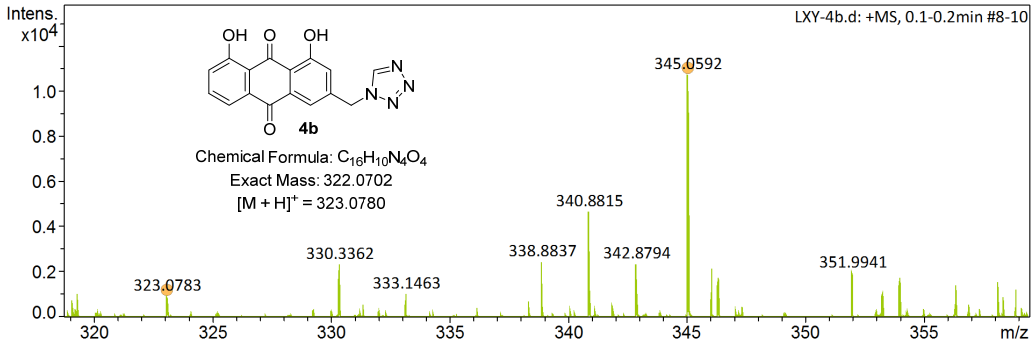

^{1}H NMR spectrum of compound **5a**

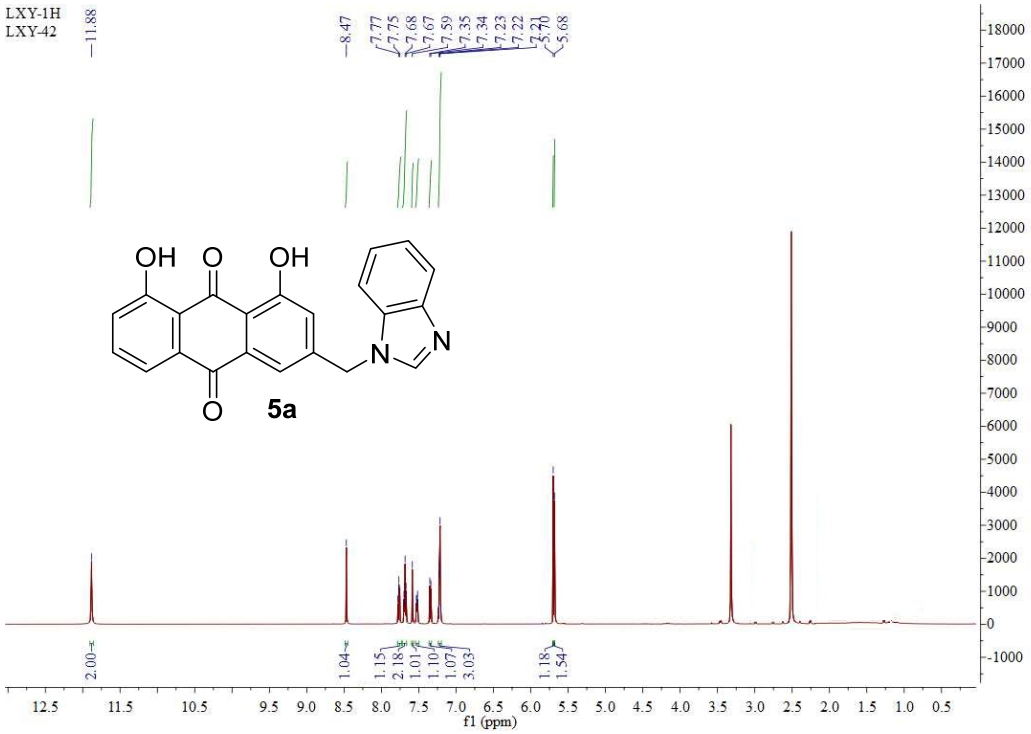

^{13}C NMR spectrum of compound **5a**

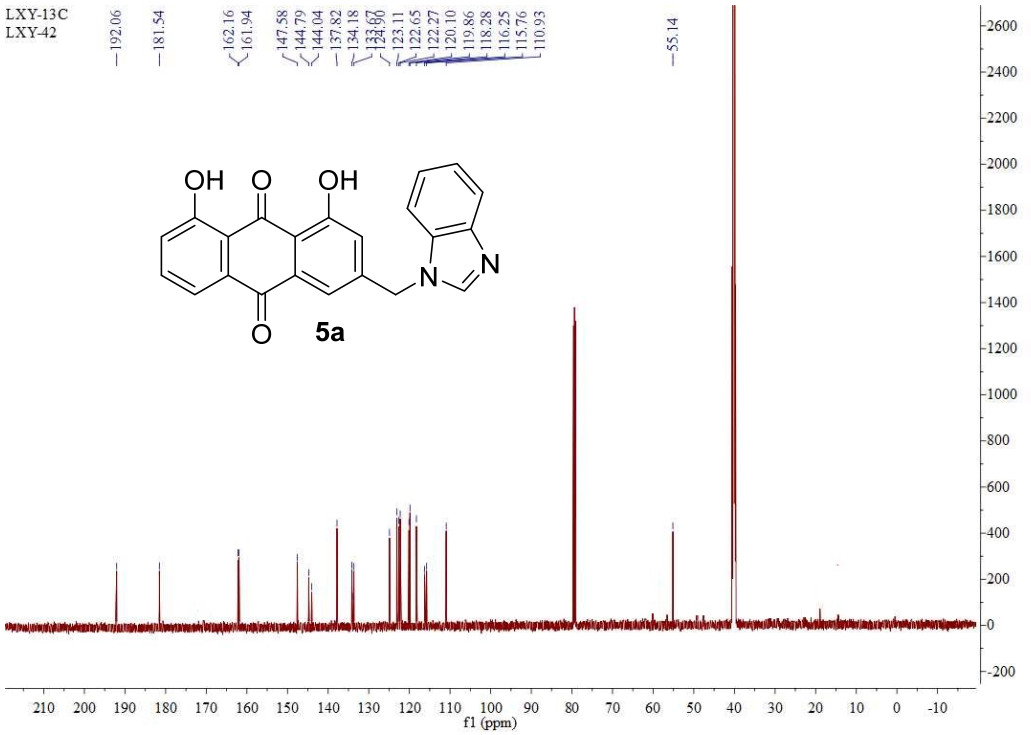

HRMS spectrum of compound **5a**

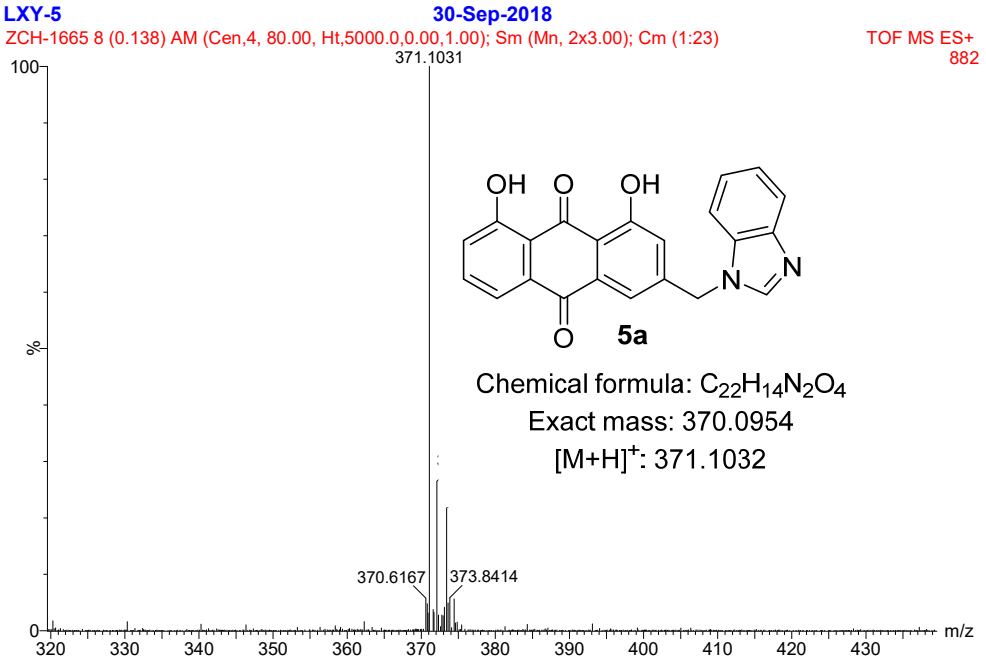

^{1}H NMR spectrum of compound **5b**

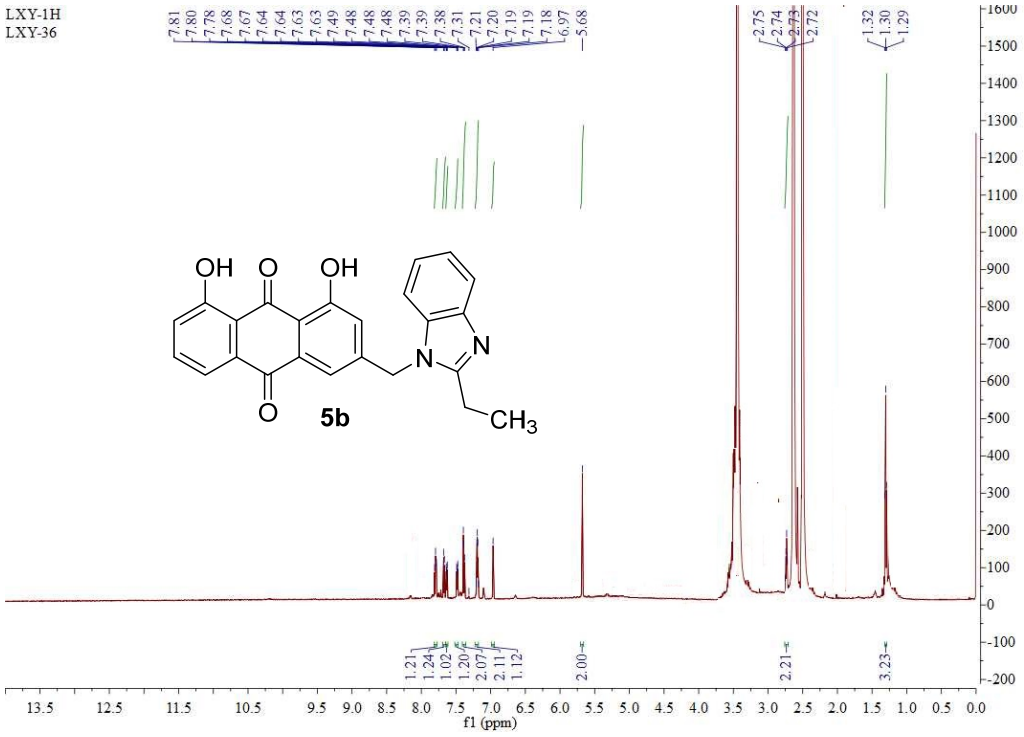

^{13}C NMR spectrum of compound **5b**

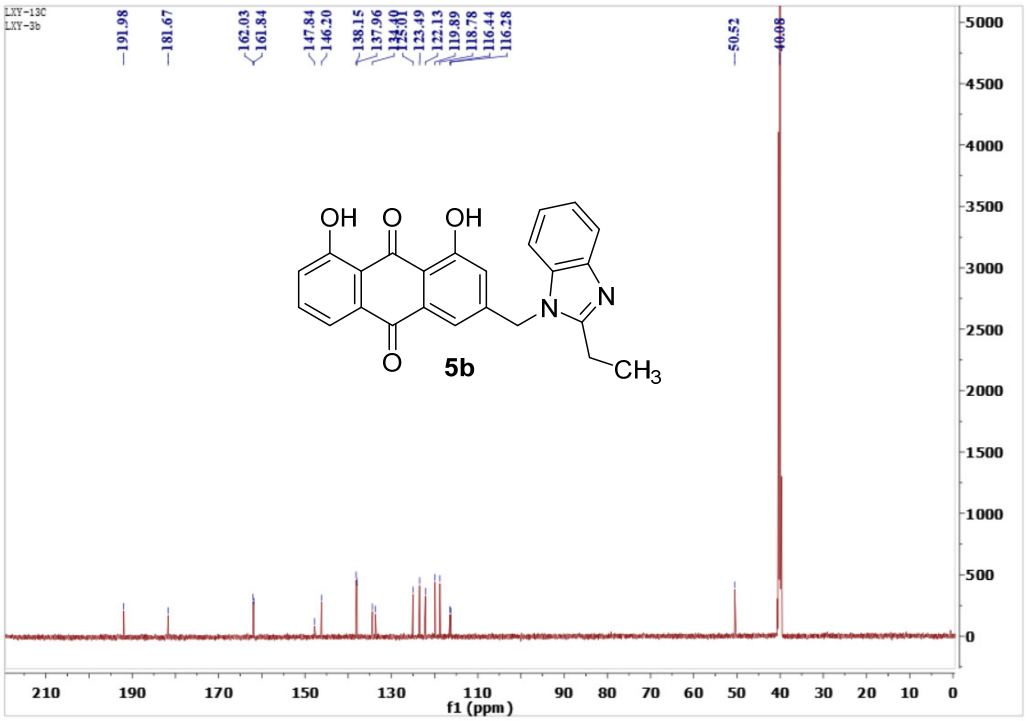

HRMS spectrum of compound **5b**

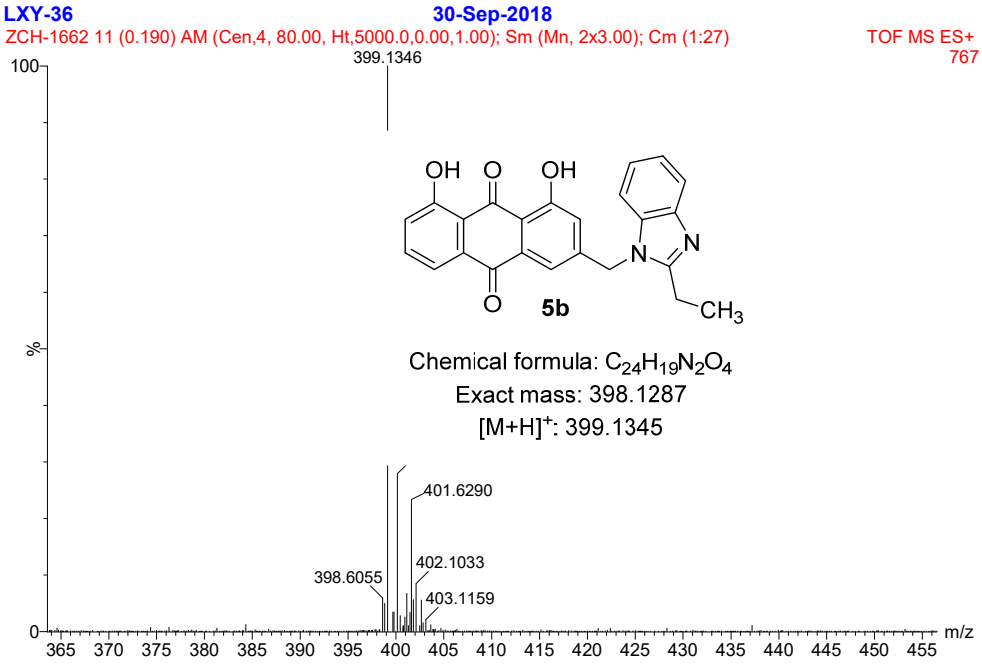

^{1}H NMR spectrum of compound **5c**

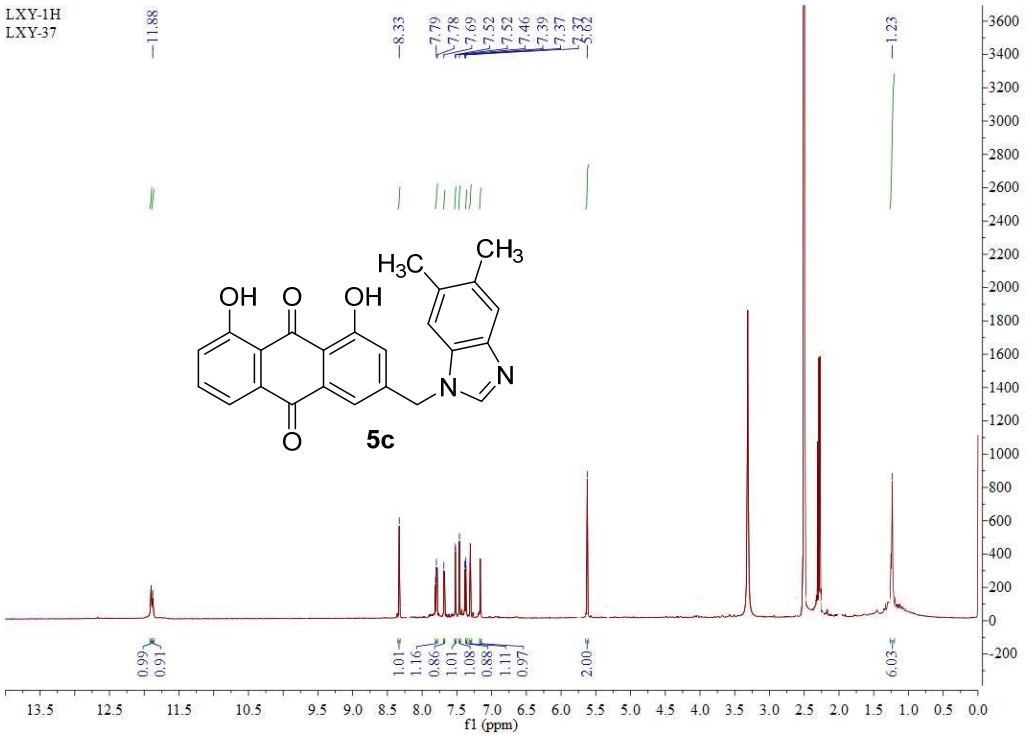

^{13}C NMR spectrum of compound **5c**

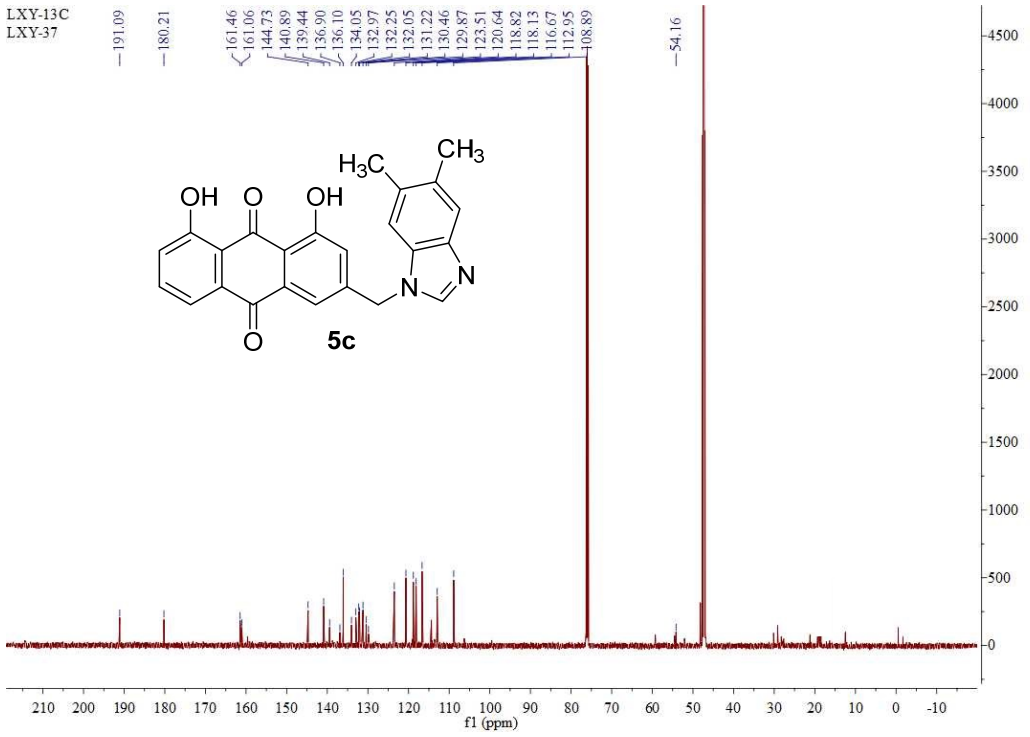

HRMS spectrum of compound **5c**

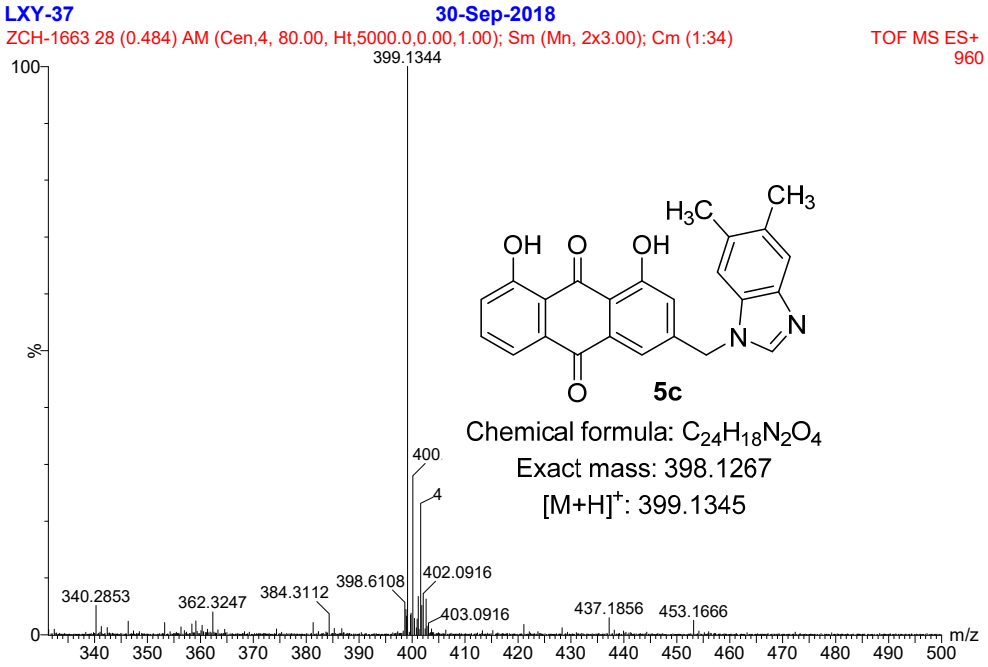

^{1}H NMR spectrum of compound **6**

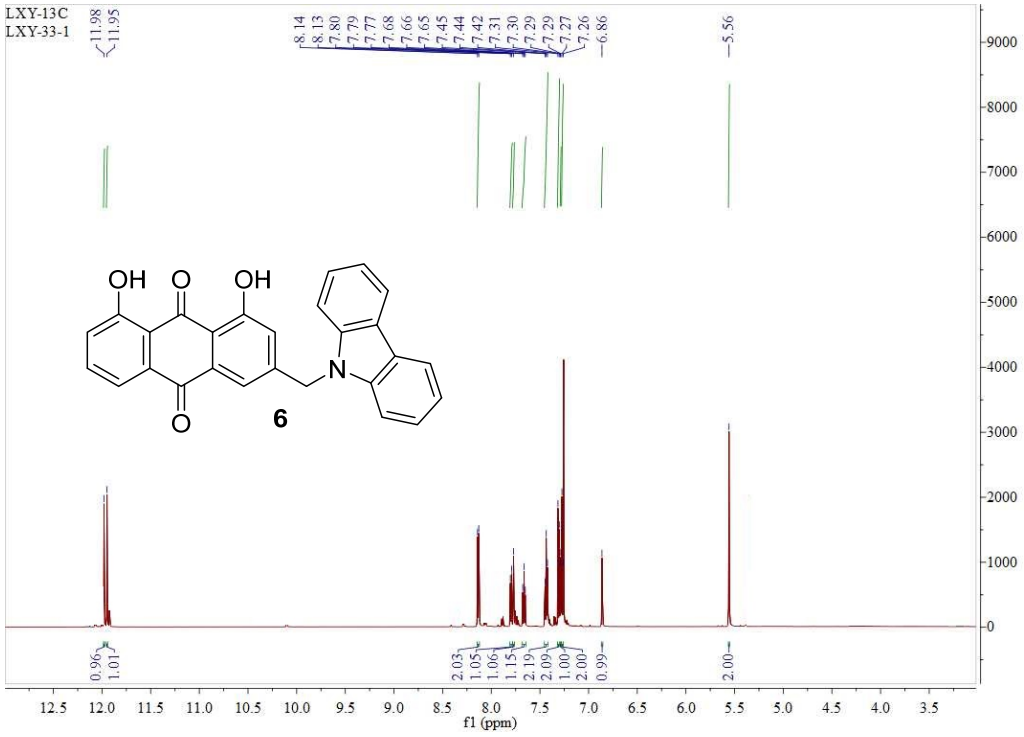

^{13}C NMR spectrum of compound **6**

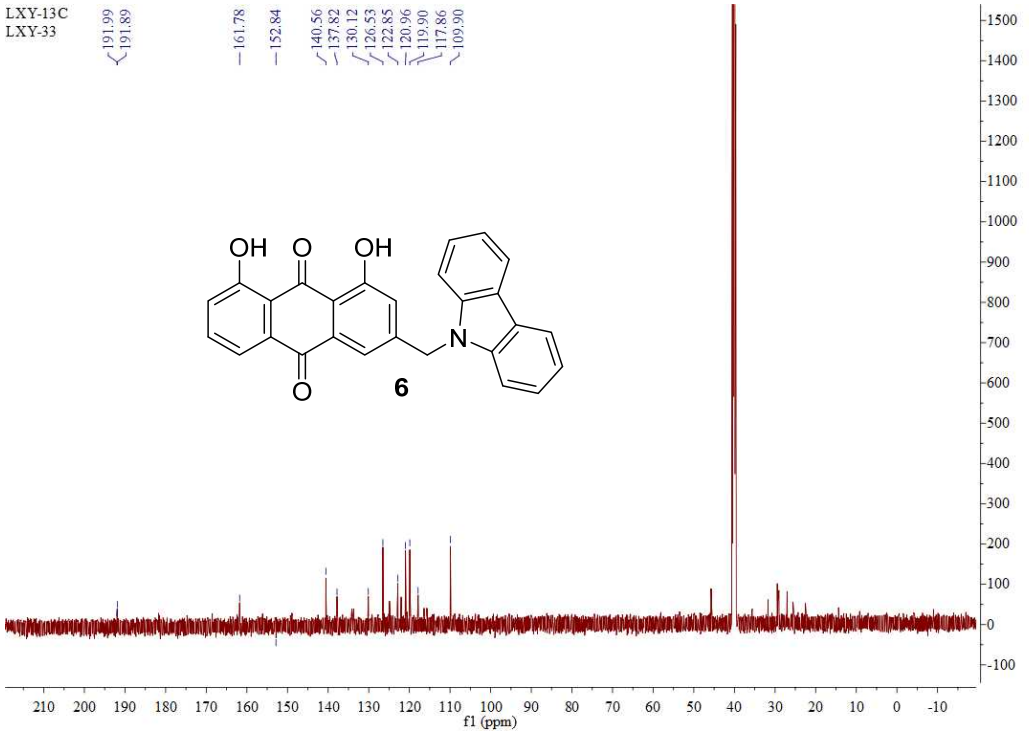

HRMS spectrum of compound **6**

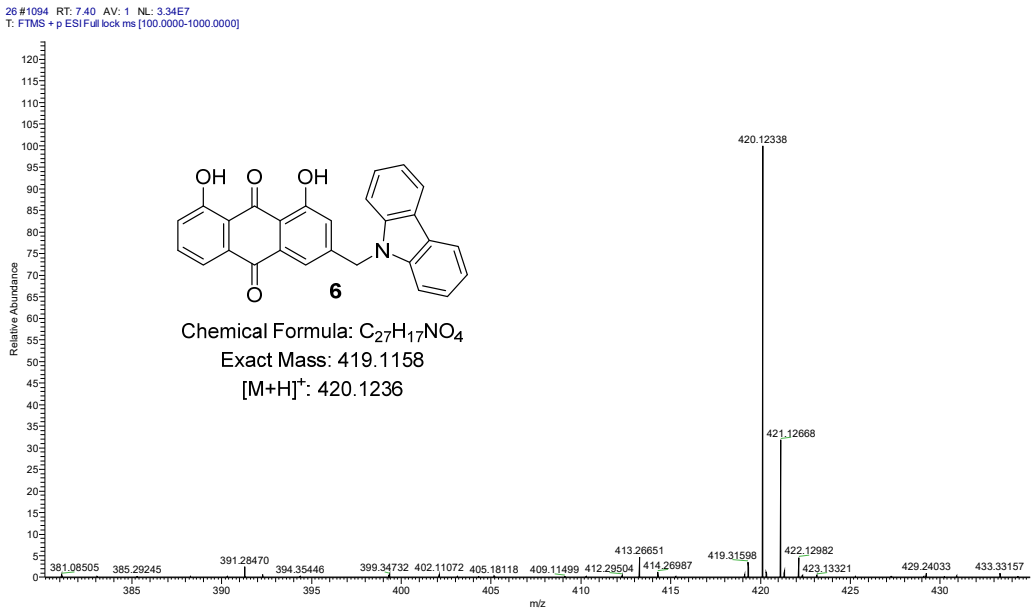

^{1}H NMR spectrum of compound **7a**

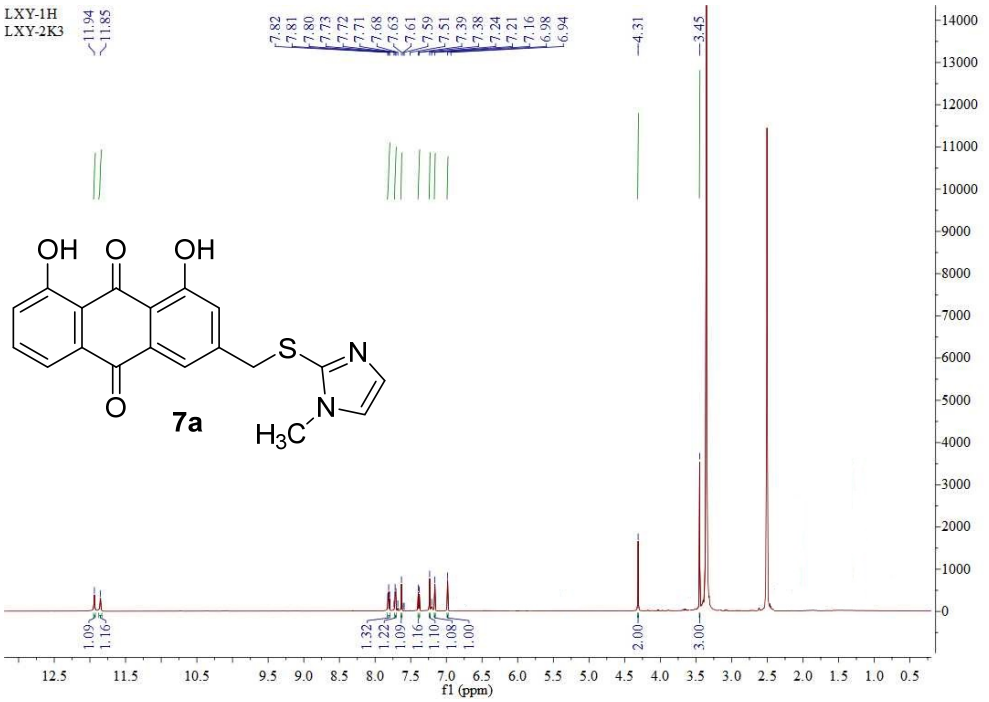

^{13}C NMR spectrum of compound **7a**

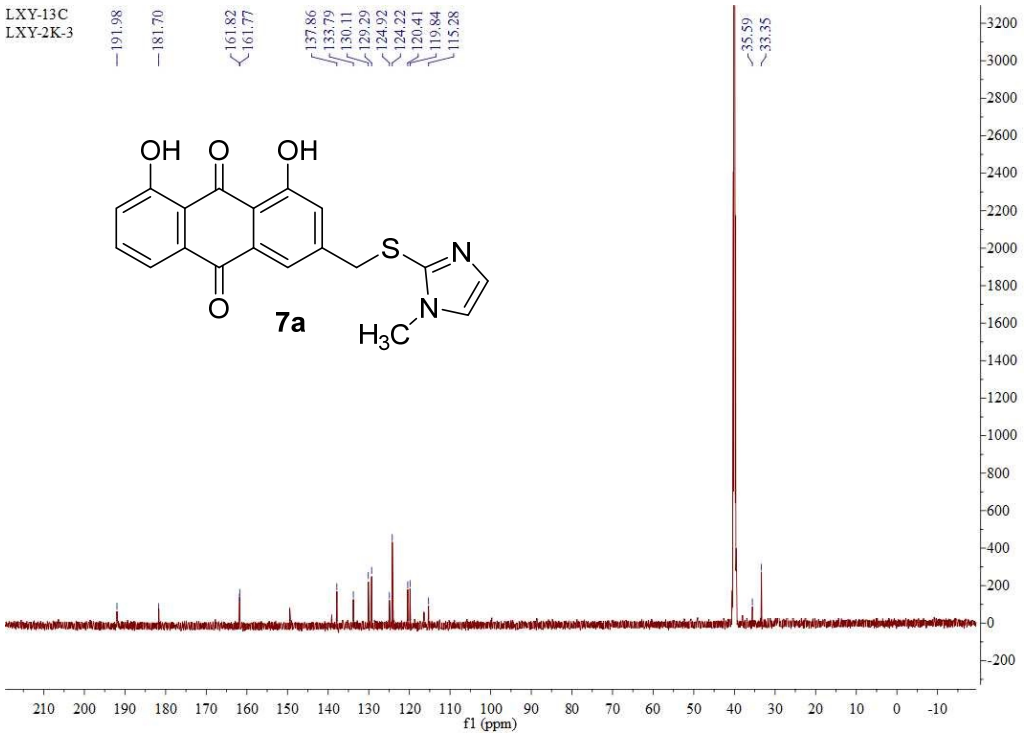

HRMS spectrum of compound **7a**

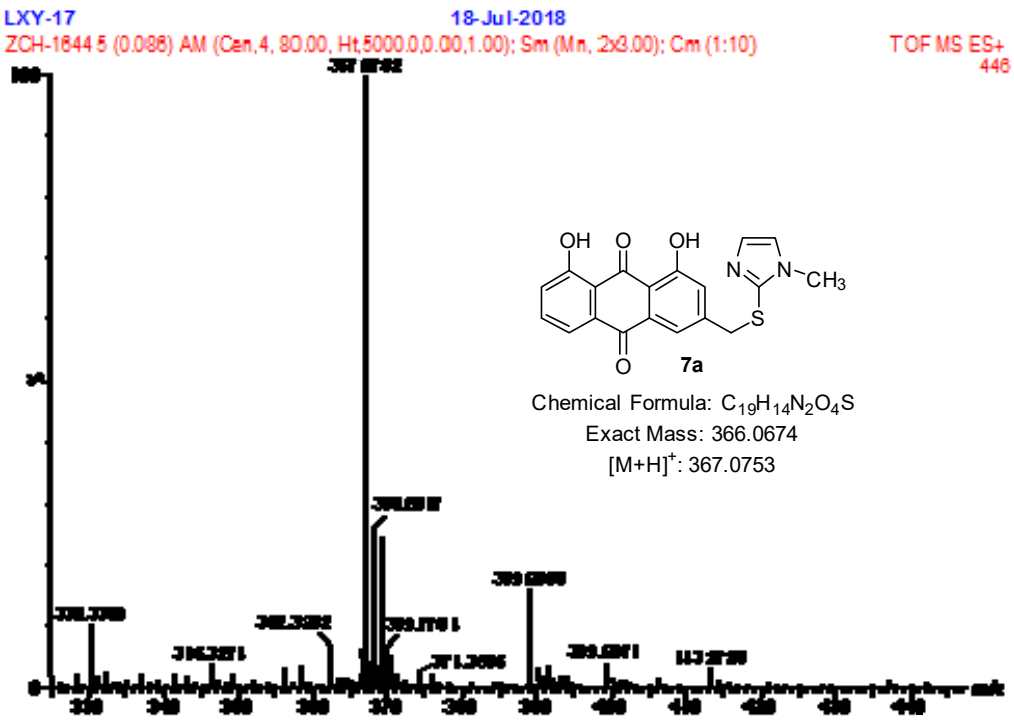
LXY-17
18-Jul-2018
ZCH-1644 5 (0.086) AM (Cen,4, 80.00, Ht,5000.0,0.00,1.00); Sm (Mn, 2x3.00); Cm (1:10)
TOF MS ES+
446
OH
O
OH
N
N
CH3
S
O
7a
Chemical Formula: C19H14N2O4S
Exact Mass: 366.0674
[M+H]+: 367.0753